NANO LETTERS

pubs.acs.org/NanoLett

Letter

Revealing the Band-Edge Exciton Fine Structure of Single InP Nanocrystals

Elise Prin,[†] Chenghui Xia,[†] Yu-Ho Won, Eunjoo Jang, Serguei V. Goupalov, Philippe Tamarat, and Brahim Lounis*

Cite This: *Nano Lett.* 2023, 23, 6067−6072

Read Online

ACCESS | Metrics & More | Article Recommendations | Supporting Information

ABSTRACT: We investigate the fundamental optical properties of single zinc-blende InP/ZnSe/ZnS nanocrystals (NCs) using frequency- and time-resolved magneto-photoluminescence spectroscopy. At liquid helium temperature, highly resolved spectral fingerprints are obtained and identified as the recombination lines of the three lowest states of the band-edge exciton fine structure. The evolutions of the photoluminescence spectra and decays under magnetic fields show evidence for a ground dark exciton level 0^L with zero angular momentum projection along the NC main elongation axis. It lies 300 to 600 μeV below the $\pm1^L$ bright exciton doublet, which is finely split by the NC shape anisotropy. These spectroscopic findings are well reproduced with a model of exciton fine structure accounting for shape anisotropy of the InP core. Our spectral fingerprints are extremely sensitive to the NC morphologies and unveil highly uniform shapes with prolate deviations of less than 3% from perfect sphericity.

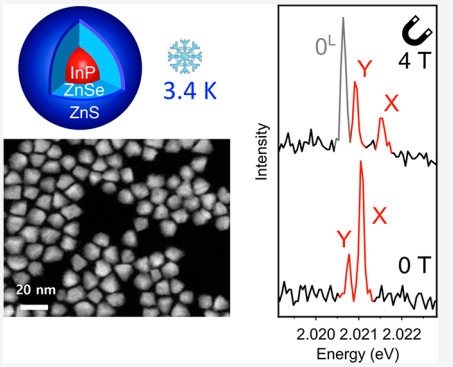

KEYWORDS: *indium phosphide nanocrystals, single-dot spectroscopy, magneto-photoluminescence, exciton fine structure*

Semiconductor nanocrystals (NCs) feature quantum confinement effects, leading to size-dependent optical properties that are ideal for tunable absorbers and emitters in various fields of applications. Historically, prototypical CdSe-based core/shell NCs were extensively studied as they offer bright luminescence through the whole visible spectrum but present major environmental and toxicity hazards. Indium phosphide (InP) NCs are a less toxic alternative to Cd-based NCs,[1−3] while possessing similar photoluminescence (PL) properties as a result of a suitable bulk band gap. They have thus quickly emerged in a variety of technological applications such as NC-based light-emitting devices,[2,4] solar cells,[5] photocatalysts,[6,7] and bioimaging.[8]

The development of applications with the integration of InP NCs requires a deep understanding of the fundamental optical properties of their band-edge excitons, whose recombination is at the origin of the luminescence. In particular, mapping the dark exciton states within the exciton fine structure is crucial in view of potential applications in quantum technologies based on the coherent manipulation of long-lived spin qubits.[9,10] In InP NCs, the electron ground $1S_e$ level is doubly degenerate with respect to its spin projection of $\pm1/2$, and the hole ground $1S_{3/2}$ level is 4-fold degenerate with respect to projections 3/2, 1/2, −1/2, and −3/2 of its total angular momentum $J = 3/2$, as for CdSe NCs.[11] The electron−hole exchange interaction[12] splits the 8-fold degenerate exciton state of spherical NCs with a cubic (zinc-blende) lattice structure into a ground optically passive (dark) 5-fold degenerate state with a total angular momentum of $F = 2$ and an upper optically active 3-fold degenerate state with $F = 1$, as depicted in Figure 1a. Breaking of the spherical symmetry in spheroidal-shaped NCs leads to five band-edge exciton sublevels $F_z = \pm2$, $\pm1^L$, $\pm1^U$, 0^L, and 0^U, where F_z is the projection of the total exciton angular momentum onto the spheroid's cylindrical z axis and the superscripts L and U respectively denote lower and upper sublevels. The ground exciton level is optically forbidden (dark), with $F_z = \pm2$ for an oblate NC or $F_z = 0^L$ for a prolate NC (Figure 1a). Pioneering spectroscopic and time-resolved studies on ensembles of InP-based core/shell NCs[13−15] suggest the presence of a ground dark exciton level located well below (∼ 5−10 meV) the lowest bright exciton level for InP NCs with a core size of ∼3 nm. These levels were respectively attributed to the ±2 and $\pm1^L$ states of oblate NCs.[14,15] However, averaging over NC sizes and shapes as well as limited spectral resolution inherent in these ensemble spectroscopic methods may hide subtle spectral features, making the assignments of the lines to the exciton fine structure states questionable. From single-dot spectroscopic measurements coupled to fluorescence line narrowing (FLN)

Received: April 18, 2023
Revised: June 15, 2023
Published: June 23, 2023

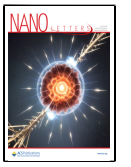

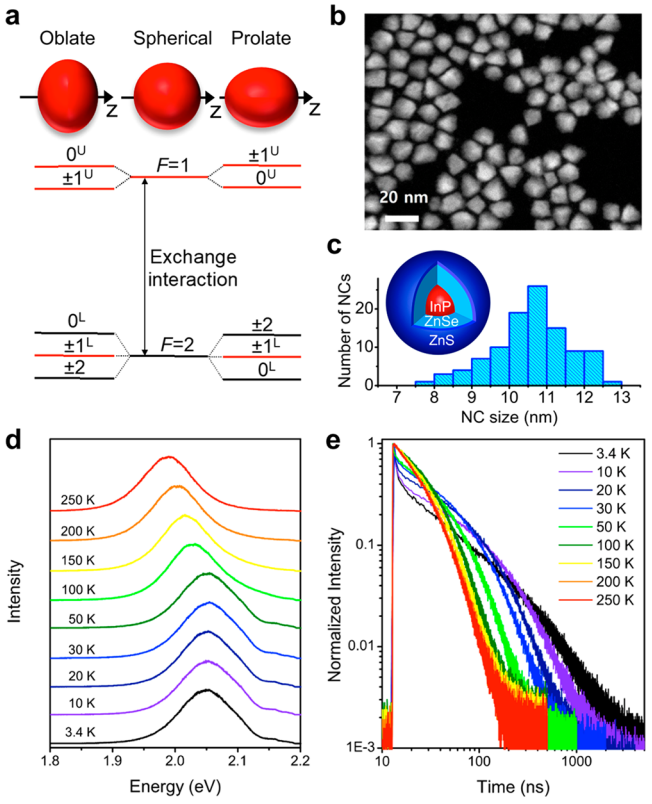

Figure 1. Characterization and ensemble optical properties of InP/ZnSe/ZnS NCs. (a) Energy-level scheme of the band-edge exciton fine structure of a zinc-blende nearly spherical InP NC. The dark levels are marked in black, and the bright ones, in red. While states ±2 and 0^L are truly dark states, states $\pm1^L$ are predicted to have a reduced (respectively zero) oscillator strength for a nearly spherical (respectively spherical) NC. (b) Transmission electron microscopy images of InP/ZnSe/ZnS NCs. (c) Schematic of the core−shell structure of these NCs and histogram of their sizes. (d) The ensemble PL spectrum and (e) the PL decay of an ensemble of InP/ZnSe/ZnS NCs are displayed for various temperatures ranging from 250 to 3.4 K.

on InP NC ensembles,[16] it was instead proposed that the band-edge exciton fine structure lies in the nearly spherical regime and that the single-NC emission lines stem from upper bright states $\pm1^U$ and 0^U located ∼6 meV above the $F = 2$ quintuplet. However, these assignments remain elusive in the absence of spectral signatures of dark- and bright-exciton recombination measured on single InP NCs.

In this work, we investigate the magneto-optical spectroscopic properties of single InP/ZnSe/ZnS core/shell/shell NCs at cryogenic temperature, which leads to unprecedented spectral fingerprints of the band-edge exciton fine structure. Using magnetic coupling between bright and dark states,[17] we show direct evidence for magnetic brightening of the dark exciton ground state, which lies only a few hundred μeV below the lowest bright exciton doublet, in sharp contrast with the previous reports.[13−16] The evolution of the PL spectra and decays with magnetic fields is well reproduced with a model of band-edge exciton fine structure accounting for InP-core shape anisotropy. We infer that the fine structure is in the prolate, nearly spherical regime and attribute the observed sublevels to the ground dark 0^L state and the $\pm1^L$ states finely split by NC shape anisotropy. Our spectroscopic results and calculations set the foundations of refined theoretical models of the exciton fine structure and its magnetic properties in these nanostructures.

The InP/ZnSe/ZnS NCs studied here are synthesized along the lines developed by Won et al.[2] They are composed of a nearly spherical zinc-blende InP core with a diameter of 3.3 nm and a thick ZnSe interlayer with a thickness of ∼3 nm that is further capped by a single layer of ZnS (thickness ∼0.4 nm). They have a polyhedron shape with an average size of ∼10.5 nm and a size polydispersity of as low as 10% (Figure 1b and c). Strong deviations from a spherical shape are observed in the TEM images due to the difficulty of growing uniform shells. Nevertheless, those epitaxial shells significantly improve the PL quantum yield through surface passivation. The absorption and emission spectra of the ensemble InP/ZnSe/ZnS NCs at room temperature are presented in Figure S1. When lowering the temperature from 250 to 3.4 K (Figure 1d), the ensemble PL spectra of these InP NCs show a blue shift down to 50 K, which is attributed to the crystal contraction.[18,19] A first evaluation of the exciton recombination dynamics in these InP NCs can be derived from the evolution of their PL decay with temperature. As shown in Figure 1e, the PL lifetime is short (∼20 ns), close to room temperature and comparable to that of prototypical CdSe NCs. The PL decay becomes multi-exponential at cryogenic temperatures, with a long component of ∼1 μs at 3.4 K. As previously observed on CdSe NCs,[20] this behavior is a signature of the thermal redistribution of population between a long-lived, ground exciton state and the neighboring bright states.

In order to investigate the band-edge exciton fine structure of these NCs at the single dot level and thus get rid of

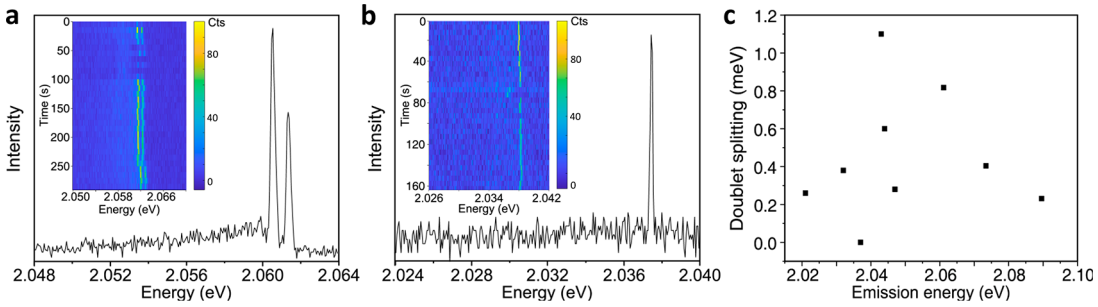

Figure 2. Bright exciton splittings in a zero magnetic field. The PL spectra (a) and (b) of two different single InP NCs show doublet and singlet emission lines at 3.5 K, respectively. Insets: Spectral trails of these NCs over time. (c) Energy splittings of spectral doublets as a function of the emission energy. The data point with quasi-degeneracy is strengthened by the evolution of the PL spectrum of this NC under magnetic fields, as shown in Figure 3c.

https://doi.org/10.1021/acs.nanolett.3c01419
Nano Lett. 2023, 23, 6067−6072

inhomogeneities in NC sizes and shapes, the NCs are dispersed in a poly(methyl methacrylate) (PMMA) thin film spin-cast on a sapphire coverslip and then photoexcited with a continuous laser with wavelength 561 nm. The sample is cooled to liquid helium temperature to reduce the population of phonons responsible for homogeneous broadening of the emission lines. At zero magnetic fields, the PL spectrum is composed of two sharp, resolution-limited lines, as exemplified in Figure 2a. The spectral trajectories of these doublets, built with consecutive PL spectra (inset of Figure 2a), show evidence of identical spectral excursions and intensity fluctuations over time. We thus infer that these lines stem from the same single NCs and attribute them to the zero-phonon recombination lines (ZPLs) of the two lowest bright exciton sublevels. As an exception (~10% of the NCs), the individual NC whose PL spectrum and spectral trail are displayed in Figure 2b presents a single ZPL in zero field. Overall, the bright exciton doublet splittings are distributed in the range from 0 to 1.1 meV and are presented in Figure 2c as a function of their exciton recombination energy. The apparent lack of correlation between these splittings and the emitted-photon energies suggests that the doublet splittings may not depend on the NC diameter but originate from NC shape anisotropy effects, as will be discussed below.

Under external magnetic fields applied in the Faraday configuration, a third line emerges on the low-energy side of the doublet and gains weight with increasing fields, as exemplified in Figure 3a and b. Other examples are presented in Figure S2 and exhibit similar behaviors. As observed in single prolate CdSe NCs[21,22] and single perovskite NCs,[23,24] the onset of a new, single ZPL under magnetic fields is the hallmark of magnetic brightening of a nondegenerate ground dark exciton level. We thus rule out the possibility that the ±2 dark level, which would split under magnetic fields,[25] is the ground exciton level in these NCs. The three ZPLs revealed by magneto-PL spectroscopy are thus assigned to the non-degenerate ground exciton state 0^L topped by the bright exciton doublet $\pm 1^L$ split by NC shape anisotropy.[22,26,27] For the NC displaying a single line in zero field (the same NC as in Figure 2b), the application of magnetic fields actually reveals that this line consists of a bright doublet with a splitting much less than the resolution limit of the spectrograph (~100 μeV), as demonstrated in Figure 3c and d. Over the studied single NCs, the energy splittings between the lowest dark exciton level and the center of the bright doublet range from 300 to 600 μeV, which is an order of magnitude less than those extracted from ensembles of InP-based QDs (~6 meV).[13−16]

The magnetic brightening of the dark ground exciton is also evidenced by the field dependence of the low-temperature PL decay of single NCs, as exemplified in Figure 4a. In zero field, the decay is biexponential with a long component (lifetime of ~400 ns) assigned to the dark exciton recombination. With increasing fields, the long-time component drastically shortens and gains weight in the PL decay. Indeed, the magnetic coupling opens a radiative recombination channel for the ground exciton via admixture in the dark state of the bright states,[23,28,29] as previously observed in CdSe single NCs.[28] The increase of the long-component decay rate Γ_L with the amplitude B of the magnetic field is displayed in Figure 4b and modeled within the framework of a two-level model accounting for the magnetically coupled 0^L and Y states (see Supporting Information, SI Note 1). In particular, we use electron and hole Landé factors $g_e = 1.55$ and $g_h = -1.5$ close

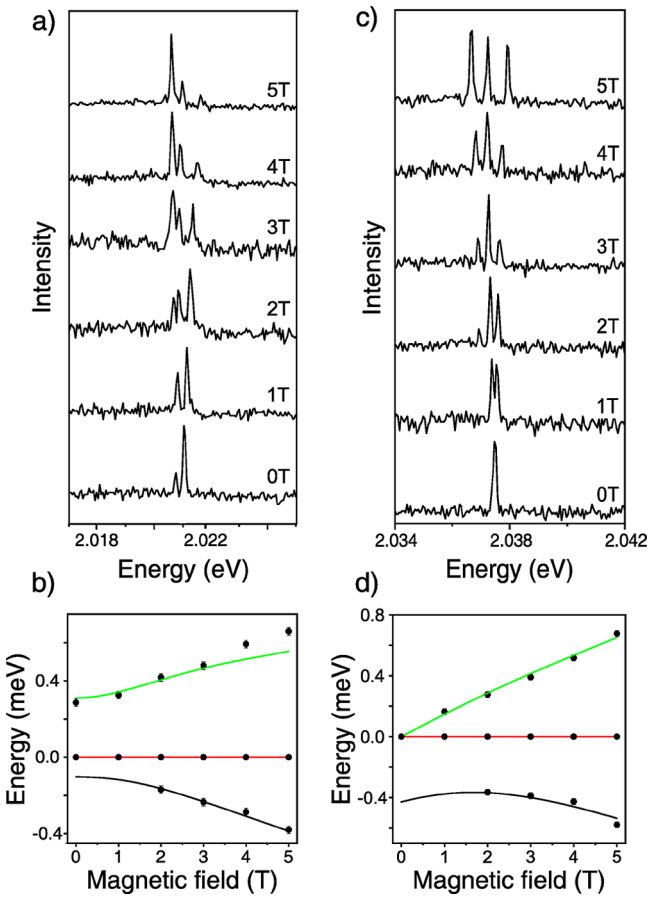

Figure 3. Magnetic brightening of the lowest dark exciton state of individual InP NCs. (a, c) Evolution of the PL spectrum of two different single NCs as a function of applied magnetic fields up to 5 T. The new line emerging on the low-energy side of the spectrum is assigned to the dark ground exciton state. The relative spectral positions of the ZPLs with respect to the ZPL assigned to the lowest bright state are respectively displayed in (b) and (d) as a function of the applied magnetic field. The fitting curves displayed in (b) and (d) are obtained using the following parameters of NC nonsphericity and magnetic field orientation: $\mu_z = 0.015$, $\mu_{xy} = 3.4 \times 10^{-3}$, and $(\theta, \varphi) = (55°, 10°)$ for (b) and $\mu_z = 0.031$, $\mu_{xy} = 0$, and $(\theta, \varphi) = (32°, 0)$ for (d), with (θ, φ) being respectively the polar and azimuthal angles.

to those calculated in a recent study,[30] as well as a common set of field orientation angles and level splittings to reproduce both the ZPL spectral shifts (Figure 4c) and the PL decay of this NC.

In order to reproduce these spectroscopic findings, we model the band-edge exciton fine structure of zinc-blende InP NCs with the Hamiltonian[11,31−33]

$$\hat{H} = -\eta(\hat{\boldsymbol{\sigma}}\cdot\hat{\boldsymbol{J}}) - \frac{\Delta}{2}\left(\hat{J}_z^2 - \frac{5}{4}\right) + \frac{C}{\sqrt{3}}(\hat{J}_x^2 - \hat{J}_y^2) + \mu_B\frac{g_e}{2}(\hat{\boldsymbol{\sigma}}\cdot\boldsymbol{B}) - \mu_B g_h(\hat{\boldsymbol{J}}\cdot\boldsymbol{B}) \quad (1)$$

where $\hat{\sigma}_\alpha$ ($\alpha = x, y, z$) are the Pauli matrices and $\hat{J}_\alpha$ represents the matrices of the angular momentum $J = 3/2$, g_e and g_h are the electron and hole effective Landé factors, μ_B is the Bohr magneton, and $\boldsymbol{B}$ is the magnetic field. The characteristic energies η, Δ, and C are calculated using the NC material and shape parameters (SI Note 2). The first term on the right-hand side of eq 1 preserves spherical symmetry and describes the

https://doi.org/10.1021/acs.nanolett.3c01419
Nano Lett. 2023, 23, 6067−6072

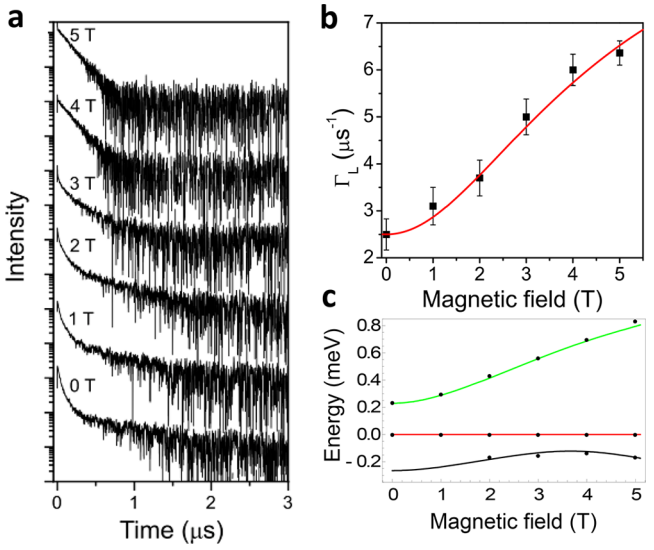

Figure 4. Evolution of the PL decay and exciton-level energies of a single NC under magnetic fields. (a) PL decay curves of a single InP NC under various magnetic fields. The corresponding PL spectra are displayed in Figure S2b. The increase in the long component decay rate Γ_L displayed in (b) is a signature of magnetic coupling of the long-lived dark exciton state with the neighboring bright states. This evolution is modeled within the framework of the magnetic coupling model described in SI Note 1 and accounts for the ground dark state and the lowest bright exciton state, having exciton recombination rates of Γ_{0^L} and Γ_Y. The PL decay and the PL spectra (c) are reproduced with a common set of parameters, using $\Gamma_Y = 0.021$ ns^{-1}, $\Gamma_{0^L} = 2.5$ μs^{-1}, $\theta = 10°$, $\varphi = 0°$, $g_e = 1.55$, and $g_h = -1.5$.

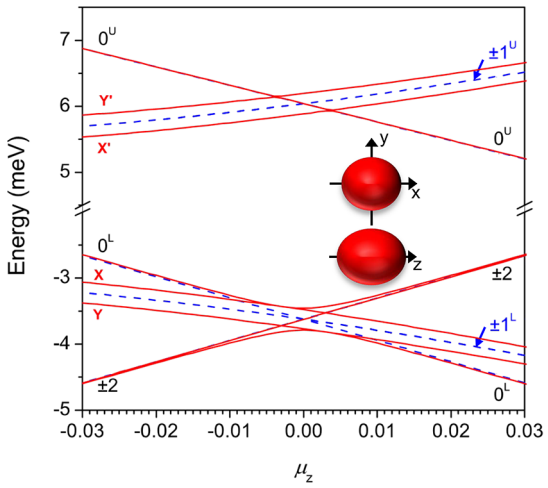

Figure 5. Band-edge exciton fine structure of a core−shell InP NC with a zinc-blende crystal structure. The band-edge exciton fine structure is calculated as a function of the NC-core aspect ratio μ_z around the region where the heavy-hole and light-hole exciton branches cross. The NC core has the same volume as a sphere with a diameter of 3.3 nm. The black dashed lines give the fine structure of a NC with no shape anisotropy in the (x, y) plane ($\mu_{xy} = 0$), while the solid red curves correspond to the case where $\mu_{xy} = 0.003$. Shape anisotropy in the (x, y) plane ($\mu_{xy} \neq 0$) introduces splittings of the $\pm1^L$ sublevel (into states denoted X and Y) and the $\pm1^U$ sublevel (into states denoted X′ and Y′) as well as complex level anticrossings within the $F = 2$ quintuplet. Inset: Illustration of the spheroidal perturbations for $\mu_z > 0$ and $\mu_{xy} > 0$.

electron−hole exchange interaction,[12,32,33] which splits the band-edge exciton into the 3-fold degenerate bright level with $F = 1$ and the 5-fold degenerate dark level with $F = 2$, as depicted in Figure 1a. The second term introduces a cylindrically symmetric perturbation resulting from a uniaxial deformation that transforms the NC shape from spherical to spheroidal.[34] As sketched in Figure 1a, this term further splits the exciton sublevels with respect to the quantum number $|F_z|$. It also mixes states $\pm1^L$ and $\pm1^U$, thus leading to the partial brightening of $\pm1^L$ (Figure 1a). The resulting energy levels for InP/ZnSe core/shell NCs are shown in Figure 5 with blue dashed lines as functions of the parameter $\mu_z = 2\frac{c-a}{c+a}$, where $a \equiv b$ and c are the semiaxes along x, y, z of the InP spheroid core having the same volume as a sphere of diameter 3.3 nm. The third term of eq 1 is responsible for further reduction of the NC shape symmetry, whereby the NC shape is stretched along the x direction and simultaneously squeezed along the y direction while preserving its elongation along the z direction.[31] It leads to splitting of the sublevels with $F_z = \pm1$ into states X and Y polarized along x and y directions in zero magnetic field. The energy levels calculated for such InP/ZnSe core/shell NCs are shown in Figure 5 with red solid lines for an x, y anisotropy parameter $\mu_{xy} = 2\frac{a-b}{a+b} = 0.003$, with a and b now being distinguished for a triaxial ellipsoid. Let us note that our choice of z for the main deformation axis of the NC shape implies that $|\mu_{xy}| \ll |\mu_z|$. The splittings due to NC shape nonsphericity are further affected by the anisotropic exchange interaction,[31] which can be neglected for the exciton quintuplet $F = 2$ with low oscillator strength. It is also worth noting that given the conduction and valence band offsets between the InP core and the ZnSe shell,[35] our calculations of the electron and hole wave functions indicate that the hole essentially resides in the core while the electron, having a much lower effective mass, is distributed over the core−shell NC (SI Note 2 and Figure S3). This effect reduces the electron−hole overlap and thus the strength η of the electron−hole exchange interaction compared to core-only InP NCs. Finally, the last two terms on the right-hand side of eq 1 account for Zeeman splitting in external magnetic fields[11] and are used to fit the experimental evolutions of the PL spectra and PL decay under increasing magnetic fields (Figure 3b and d and Figure 4b and c).

In light of the energy-level diagrams of Figure 5, our spectroscopic findings over a variety of single NCs show evidence that the magnetically brightened exciton state is the nondegenerate ground dark 0^L state, which points to a prolate regime of the InP cores, i.e., $\mu_z > 0$. Moreover, the bright−dark splittings ranging from 300 to 600 μeV are consistent with the fine structure regime of slightly prolate NCs with $\mu_z < 0.03$. The X−Y splittings with average ∼400 μeV point to a tiny shape anisotropy in the (x, y) plane with average $\mu_{xy} \approx 0.003$. These results highlight the power of single-NC spectroscopy to unveil subtle deviations in NC morphologies and confirm that the InP NC cores prepared with this synthesis method[2] are highly uniform and almost spherical.

In conclusion, our magneto-PL investigations of single InP/ZnSe/ZnS reveal highly resolved spectral fingerprints of the three lowest exciton fine structure states. We provide evidence that they stem from the recombination of the ground dark exciton 0^L and the lowest bright $\pm1^L$ states, whose degeneracy is lifted by the NC shape anisotropy. The 0^L ground state seems to be a truly dark state from which luminescence is evidenced only under magnetic fields, as in prolate CdSe NCs.[21] The evolutions of the energy levels and PL decays with

https://doi.org/10.1021/acs.nanolett.3c01419
Nano Lett. 2023, 23, 6067−6072

applied magnetic fields are well reproduced with a model of band-edge exciton fine structure accounting for the InP core shape anisotropy. Interestingly, our findings and modeling allow an alternative interpretation of the previous FLN experiments performed on an ensemble of similar NCs.[14,15] Indeed, in FLN spectroscopy, the monochromatic laser resonantly excites a small subensemble of the NCs to the bright states of the exciton branch F = 1. After rapid nonradiative relaxation to the lowest branch F = 2, the emission stems from states $\pm 1^{L}$ having weaker oscillator strengths. The reported shifts (5−10 meV) between the excitation photon energy and the narrow PL line correspond to the splitting between branches F = 1 and F = 2, in accordance with our calculations of the fine structure. Our single-NC spectroscopic study and calculations will also guide the development of refined theoretical models to describe the physical properties of these emerging nanostructures. Further investigations will aim at exploring the signatures of the recombination of other charge complexes such as trions and the biexciton in InP NCs, with a view to investigating the suitability of these systems as quantum light sources.

■ ASSOCIATED CONTENT

Supporting Information

The Supporting Information is available free of charge at https://pubs.acs.org/doi/10.1021/acs.nanolett.3c01419.

Room-temperature absorption and PL spectra of ensemble InP/ZnSe/ZnS NCs, magnetic brightening of the lowest dark exciton state of various single InP NCs, model of PL decay as a function of the amplitude of the magnetic field, and modelization of the electron−hole exchange interaction (PDF)

■ AUTHOR INFORMATION

Corresponding Author

Brahim Lounis − *Université de Bordeaux, LP2N, Talence F-33405, France; Institut d'Optique and CNRS, LP2N, Talence F-33405, France;* orcid.org/0000-0001-7501-0236; Email: brahim.lounis@u-bordeaux.fr

Authors

Elise Prin − *Université de Bordeaux, LP2N, Talence F-33405, France; Institut d'Optique and CNRS, LP2N, Talence F-33405, France*

Chenghui Xia − *Université de Bordeaux, LP2N, Talence F-33405, France; Institut d'Optique and CNRS, LP2N, Talence F-33405, France;* orcid.org/0000-0001-5087-8805

Yu-Ho Won − *Samsung Advanced Institute of Technology, Samsung Electronics, Suwon 16678, South Korea;* orcid.org/0000-0002-6065-7800

Eunjoo Jang − *Samsung Advanced Institute of Technology, Samsung Electronics, Suwon 16678, South Korea;* orcid.org/0000-0003-2573-0176

Serguei V. Goupalov − *Ioffe Institute, St. Petersburg 194021, Russia; Department of Physics, Jackson State University, Jackson, Mississippi 39217, United States;* orcid.org/0000-0002-4913-0792

Philippe Tamarat − *Université de Bordeaux, LP2N, Talence F-33405, France; Institut d'Optique and CNRS, LP2N, Talence F-33405, France*

Complete contact information is available at: https://pubs.acs.org/10.1021/acs.nanolett.3c01419

Author Contributions

†E.P. and C.X. contributed equally to this work

Notes

The authors declare no competing financial interest.

■ ACKNOWLEDGMENTS

We acknowledge the financial support from the French National Agency for Research, Région Aquitaine, Idex Bordeaux (Research Program GPR Light), the EUR Light S&T, and the Samsung Global Research Outreach Program SINQUADOT (GRO project no. IO201120-07752-01). B.L. acknowledges the Institut Universitaire de France. The work of S.V.G. was supported by the NSF through DMR-2100248.

■ REFERENCES

(1) Brunetti, V.; Chibli, H.; Fiammengo, R.; Galeone, A.; Malvindi, M. A.; Vecchio, G.; Cingolani, R.; Nadeau, J. L.; Pompa, P. P. InP/ZnS as a safer alternative to CdSe/ZnS core/shell quantum dots: in vitro and in vivo toxicity assessment. *Nanoscale* **2013**, *5*, 307−317.

(2) Won, Y.-H.; Cho, O.; Kim, T.; Chung, D.-Y.; Kim, T.; Chung, H.; Jang, H.; Lee, J.; Kim, D.; Jang, E. Highly efficient and stable InP/ZnSe/ZnS quantum dot light-emitting diodes. *Nature* **2019**, *575*, 634−638.

(3) Yadav, R.; Kwon, Y.; Rivaux, C.; Saint-Pierre, C.; Ling, W. L.; Reiss, P. Narrow Near-Infrared Emission from InP QDs Synthesized with Indium(I) Halides and Aminophosphine. *J. Am. Chem. Soc.* **2023**, *145*, 5970−5981.

(4) Shirasaki, Y.; Supran, G. J.; Bawendi, M. G.; Bulović, V. Emergence of colloidal quantum-dotlight-emitting technologies. *Nature Photonics* **2013**, *7*, 13−23.

(5) Crisp, R. W.; Kirkwood, N.; Grimaldi, G.; Kinge, S.; Siebbeles, L. D. A.; Houtepen, A. J. Highly Photoconductive InP Quantum Dots Films and Solar Cells. *ACS Appl. Energy Mater.* **2018**, *1*, 6569−6576.

(6) Chakraborty, I. N.; Roy, S.; Devatha, G.; Rao, A.; Pillai, P. P. InP/ZnS Quantum Dots as Efficient Visible-Light Photocatalysts for Redox and Carbon−Carbon Coupling Reactions. *Chem. Mater.* **2019**, *31*, 2258−2262.

(7) Yu, S.; Fan, X.-B.; Wang, X.; Li, J.; Zhang, Q.; Xia, A.; Wei, S.; Wu, L.-Z.; Zhou, Y.; Patzke, G. R. Efficient photocatalytic hydrogen evolution withligand engineered all-inorganic InP and InP/ZnS colloidal quantum dots. *Nature Communications* **2018**, *9*, 4009.

(8) Zhang, L.; Yang, X.-Q.; An, J.; Zhao, S.-D.; Zhao, T.-Y.; Tan, F.; Cao, Y.-C.; Zhao, Y.-D. In vivo tumor active cancer targeting and CT-fluorescence dual-modal imaging with nanoprobe based on gold nanorods and InP/ZnS quantum dots. *J Mater Chem B* **2018**, *6*, 2574−2583.

(9) Poem, E.; Kodriano, Y.; Tradonsky, C.; Lindner, N. H.; Gerardot, B. D.; Petroff, P. M.; Gershoni, D. Accessing the dark exciton with light. *Nature Physics* **2010**, *6*, 993−997.

(10) Schwartz, I.; Cogan, D.; Schmidgall, E. R.; Don, Y.; Gantz, L.; Kenneth, O.; Lindner, N. H.; Gershoni, D. Deterministic generation of a cluster state of entangled photons. *Science* **2016**, *354*, 434−437.

(11) Efros, A.; Rosen, M.; Kuno, M.; Nirmal, M.; Norris, D.; Bawendi, M. Band-edge exciton in quantum dots of semiconductors with a degenerate valence band: Dark and bright exciton states. *Phys. Rev., B Condens. Matter* **1996**, *54*, 4843−4856.

(12) Sercel, P. C.; Efros, A. L. Band-Edge Exciton in CdSe and Other II−VI and III−V Compound Semiconductor Nanocrystals − Revisited. *Nano Letters* **2018**, *18*, 4061−4068.

(13) Biadala, L.; Siebers, B.; Beyazit, Y.; Tessier, M. D.; Dupont, D.; Hens, Z.; Yakovlev, D. R.; Bayer, M. Band-Edge Exciton Fine Structure and Recombination Dynamics in InP/ZnS Colloidal Nanocrystals. *ACS Nano* **2016**, *10*, 3356−3364.

(14) Brodu, A.; Ballottin, M. V.; Buhot, J.; van Harten, E. J.; Dupont, D.; La Porta, A.; Prins, P. T.; Tessier, M.; Versteegh, M. A. M.;

Zwiller, V.; Bals, S.; Hens, Z.; Rabouw, F. T.; Christianen, P. C. M.; de Mello Donega, C.; Vanmaekelbergh, D. Exciton Fine Structure and Lattice Dynamics in InP/ZnSe Core/Shell Quantum Dots. *ACS Photonics* **2018**, *5*, 3353−3362.
(15) Brodu, A.; Ballottin, M. V.; Buhot, J.; Dupont, D.; Tessier, M.; Hens, Z.; Rabouw, F. T.; Christianen, P. C. M.; de Mello Donega, C.; Vanmaekelbergh, D. Exciton-phonon coupling in InP quantum dots with ZnS and (Zn, Cd) Se shells. *Physical Review B* **2020**, *101*, 125413.
(16) Brodu, A.; Chandrasekaran, V.; Scarpelli, L.; Buhot, J.; Masia, F.; Ballottin, M. V.; Severijnen, M.; Tessier, M. D.; Dupont, D.; Rabouw, F. T.; Christianen, P. C. M.; de Mello Donega, C.; Vanmaekelbergh, D.; Langbein, W.; Hens, Z. Fine Structure of Nearly Isotropic Bright Excitons in InP/ZnSe Colloidal Quantum Dots. *J. Phys. Chem. Lett.* **2019**, *10*, 5468−5475.
(17) Bayer, M.; Ortner, G.; Stern, O.; Kuther, A.; Gorbunov, A. A.; Forchel, A.; Hawrylak, P.; Fafard, S.; Hinzer, K.; Reinecke, T. L.; Walck, S. N.; Reithmaier, J. P.; Klopf, F.; Schäfer, F. Fine structure of neutral and charged excitons in self-assembled In(Ga)As/(Al)GaAs quantum dots. *Physical Review B* **2002**, *65*, 195315.
(18) Varshni, Y. P. Temperature dependence of the energy gap in semiconductors. *Physica* **1967**, *34*, 149−154.
(19) Pässler, R. Basic Model Relations for Temperature Dependencies of Fundamental Energy Gaps in Semiconductors. *Phys. Status Solidi B* **1997**, *200*, 155−172.
(20) Labeau, O.; Tamarat, P.; Lounis, B. Temperature Dependence of the Luminescence Lifetime of Single CdSe/ZnS Quantum Dots. *Phys. Rev. Lett.* **2003**, *90*, 257404.
(21) Fernée, M. J.; Tamarat, P.; Lounis, B. Cryogenic Single-Nanocrystal Spectroscopy: Reading the Spectral Fingerprint of Individual CdSe Quantum Dots. *J. Phys. Chem. Lett.* **2013**, *4*, 609−618.
(22) Sinito, C.; Fernée, M. J.; Goupalov, S. V.; Mulvaney, P.; Tamarat, P.; Lounis, B. Tailoring the Exciton Fine Structure of Cadmium Selenide Nanocrystals with Shape Anisotropy and Magnetic Field. *ACS Nano* **2014**, *8*, 11651−11656.
(23) Tamarat, P.; Bodnarchuk, M. I.; Trebbia, J.-B.; Erni, R.; Kovalenko, M. V.; Even, J.; Lounis, B. The ground exciton state of formamidinium lead bromide perovskite nanocrystals is a singlet dark state. *Nat. Mater.* **2019**, *18*, 717−724.
(24) Tamarat, P.; Hou, L.; Trebbia, J.-B.; Swarnkar, A.; Biadala, L.; Louyer, Y.; Bodnarchuk, M. I.; Kovalenko, M. V.; Even, J.; Lounis, B. The dark exciton ground state promotes photon- pair emission in individual perovskite nanocrystals. *Nature Communications* **2020**, *11*, 6001.
(25) Biadala, L.; Louyer, Y.; Tamarat, P.; Lounis, B. Band-Edge Exciton Fine Structure of Single CdSe/ZnS Nanocrystals in External Magnetic Fields. *Phys. Rev. Lett.* **2010**, *105*, 157402.
(26) Htoon, H.; Furis, M.; Crooker, S. A.; Jeong, S.; Klimov, V. I. Linearly polarized "fine structure" of the bright exciton state in individual CdSe nanocrystal quantum dots. *Physical Review B* **2008**, *77*, 035328.
(27) Htoon, H.; Crooker, S. A.; Furis, M.; Jeong, S.; Efros, A. L.; Klimov, V. I. Anomalous Circular Polarization of Photoluminescence Spectra of Individual CdSe Nanocrystals in an Applied Magnetic Field. *Phys. Rev. Lett.* **2009**, *102*, 017402.
(28) Louyer, Y.; Biadala, L.; Trebbia, J. B.; Fernée, M. J.; Tamarat, P.; Lounis, B. Efficient Biexciton Emission in Elongated CdSe/ZnS Nanocrystals. *Nano Letters* **2011**, *11*, 4370−4375.
(29) Gandil, M.; Matsuda, K.; Lounis, B.; Tamarat, P. Spectroscopic signatures of spin-orbit coupling and free excitons in individual suspended carbon nanotubes. *Physical Review B* **2019**, *100*, No. 081411(R).
(30) Semina, M. A.; Golovatenko, A. A.; Rodina, A. V. Influence of the spin-orbit split-off valence band on the hole *g* factor in semiconductor nanocrystals. *Physical Review B* **2021**, *104*, 205423.
(31) Goupalov, S. V. Anisotropy-induced exchange splitting of exciton radiative doublet in CdSe nanocrystals. *Physical Review B* **2006**, *74*, 113305.
(32) Gupalov, S. V.; Ivchenko, E. L. The Fine Structure of Excitonic Levels in CdSe Nanocrystals. *Phys. Solid State* **2000**, *42*, 2030−2038.
(33) Goupalov, S. V.; Ivchenko, E. L. Electron-hole long-range exchange interaction in semiconductor quantum dots. *J. Cryst. Growth* **1998**, *184-185*, 393−397.
(34) Efros, A. L.; Rodina, A. V. Band-edge absorption and luminescence of nonspherical nanometer-size crystals. *Phys. Rev., B Condens. Matter* **1993**, *47*, 10005−10007.
(35) Toufanian, R.; Piryatinski, A.; Mahler, A. H.; Iyer, R.; Hollingsworth, J. A.; Dennis, A. M. Bandgap Engineering of Indium Phosphide-Based Core/Shell Heterostructures Through Shell Composition and Thickness. *Frontiers in Chemistry* **2018**, *6*, DOI: 10.3389/fchem.2018.00567.

https://doi.org/10.1021/acs.nanolett.3c01419
Nano Lett. 2023, 23, 6067−6072